

# Water transport through hydrophobic micro/nanoporous filtration membranes on different scales

Mian Wang<sup>1</sup> and Yongbin Zhang\*<sup>2</sup>

<sup>1</sup>School of Electronic Engineering, Changzhou College of Information Technology, Changzhou, 213164, Jiangsu Province, China

<sup>2</sup>College of Mechanical Engineering, Changzhou University, Changzhou, 213164, Jiangsu Province, China

(Received August 4, 2022, Revised October 12, 2022, Accepted November 14, 2022)

**Abstract.** Theoretical calculation results are presented for the enhancement of the water mass flow rate through the hydrophobic micro/nano pores in the membrane respectively on the micrometer and nanometer scales. The water-pore wall interfacial slippage is considered. When the pore diameter is critically low (less than 1.82nm), the water flow in the nanopore is non-continuum and described by the nanoscale flow equation; Otherwise, the water flow is essentially multiscale consisting of both the adsorbed boundary layer flow and the intermediate continuum water flow, and it is described by the multiscale flow equation. For no wall slippage, the calculated water flow rate through the pore is very close to the classical hydrodynamic theory calculation if the pore diameter ( $d$ ) is larger than 1.0nm, however it is considerably smaller than the conventional calculation if  $d$  is less than 1.0nm because of the non-continuum effect of the water film. When the driving power loss on the pore is larger than the critical value, the wall slippage occurs, and it results in the different scales of the enhancement of the water flow rate through the pore which are strongly dependent on both the pore diameter and the driving power loss on the pore. Both the pressure drop and the critical power loss on the pore for starting the wall slippage are also strongly dependent on the pore diameter.

**Keywords:** hydrophobic wall; mass transfer; membrane; multiscale; nanopore; wall slippage

## 1. Introduction

Super filtration of water has been developed fast and it relies on the use of nanoporous filtration membranes, which are often made of carbon, silica, silicon nitride, boron nitride, silicon carbonized and graphene etc (Azamat 2021, Borg and Reese 2017, Dai *et al.* 2016, Das *et al.* 2021, Holt *et al.* 2006, Majumder *et al.* 2005, Qin *et al.* 2011, Radhal *et al.* 2016). It has been observed that water flows ultra fast in the hydrophobic filtration nanopores with the diameter on the 1nm scale such as made of carbon, graphene and silicon carbonized etc (Gruener *et al.* 2016, Holt *et al.* 2006, Itoh *et al.* 2022, Kannam *et al.* 2013, Majumder *et al.* 2005, Qin *et al.* 2011, Radhal *et al.* 2016). Recent experiments even showed that the water flux through the nanopores with the diameters between 0.9nm and 1.9nm and possessing a densely fluorinated interior surface was two orders higher than that in the carbon nanotube (Itoh *et al.* 2022). These phenomena are unexplainable from classical hydrodynamic flow theory.

Experiments detected the ultra fast water flow through carbon nanotubes with several orders higher than the classical hydrodynamic theory calculation (Holt *et al.* 2006, Majumder *et al.* 2005, Qin *et al.* 2011). However, different people gave different water flow enhancement results. Majumder *et al.* (2005) showed the enhancement of 4 to 5 orders, Holt *et al.* (2006) got the enhancement of 2 to 4

orders, while Qin *et al.* (2011) gave the enhancement factor lower than 1000. These researches used the similar nanotube diameters but the very different nanotube lengths. It was typically agreed that the unexpectedly fast water flow in carbon nanotubes should be due to the water slippage on the hydrophobic nanotube wall (Mattia and Calabro 2012, Myers 2011, Whitby and Quirke 2007). The divergence among the above experimentally observed enhancement of the water flow was ascribed by Walther *et al.* (2013) to the entry and exit pressure losses, the effect of which is significantly influenced by the nanotube length.

Molecular dynamics simulations (MDS) were also done for the water flow in carbon nanotubes with different lengths (Calabrò *et al.* 2013, Rito *et al.* 2014, Thomas and McGaughey 2008). Some of them obtained the flow enhancement factors similar to the experimental results and attributed the event to the reduced friction of the carbon nanotube wall (Rito *et al.* 2014), while others gave the flow enhancement factors several orders lower than the experimental results (Thomas and McGaughey 2008). In itself, MDS is difficult to implement for long nanotubes because of the computational capacity. Multiscale approaches were also used to calculate the water flow rates through longer nanotubes. Borg and Reese (2017) used the hybrid multiscale scheme to calculate the water flow rate through the carbon nanotube with the diameters below 2nm and the lengths covering from 10nm to 1mm. They showed the flow enhancement factor is heavily dependent on the nanotube length and reaches the maximum when the nanotube length is over 0.1mm. However, their results are still apparently different from the experimental results of

\*Corresponding author, Professor,  
E-mail: engmechl@sina.com

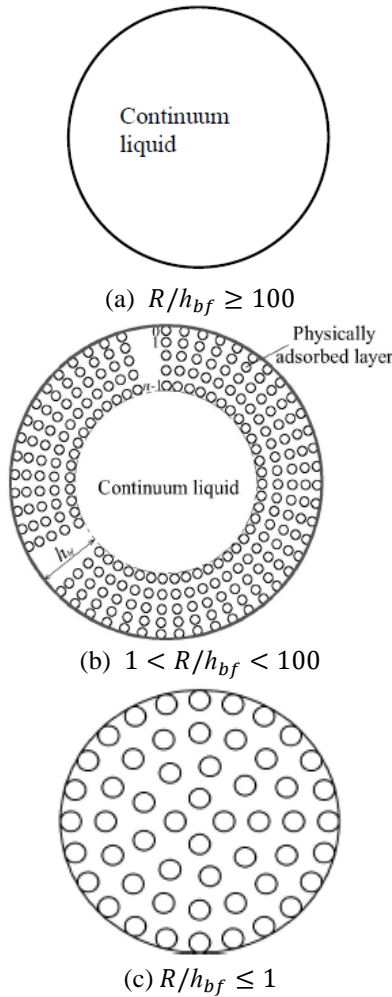


Fig. 1 Water flow in cylindrical tubes with different flow regimes. (a) Continuum flow; (b) Multiscale flow; (c) Non-continuum nanoscale flow (Li and Zhang 2021)

Holt *et al.* (2006) and Qin *et al.* (2011) for the same nanotube lengths.

In the present study, by using the closed-form explicit flow equations for the non-continuum nanoscale flow and the multiscale flow, we calculated the enhancement factor of the water flow through the carbon nanotubes with the diameters varying from 0.6nm to 2000nm. The water-pore wall interfacial slippage is considered and related to the power loss on the whole pore for driving the flow. The entry and exit pressure losses are neglected. The calculation results are thus for sufficiently long nanotube lengths. Our results show that in the case of the wall slippage, when the pore diameter is less than 1.8nm and the water flow is thus non-continuum, the calculated flow enhancement factors range between  $10^1$  and  $10^{10}$  covering the previous experimental results, and they are heavily determined by the power loss on the whole nanopore driving the flow; when the pore diameter is over 2.0nm and thus the water flow is essentially multiscale consisting of both the non-continuum adsorbed layer flow and the continuum water flow (Atkas and Aluru 2002, Yen *et al.* 2007), for a given power loss on the pore the flow enhancement factor is rapidly reduced with the increase of the pore diameter and it is several

orders lower than that for the pore diameter below 1.8nm when the pore diameter is on the scale of 1000nm.

## 2. Water flow in micro/nano pores with different flow regimes

It has been proposed that for the water flow in the micro/nano pores with different diameters, the flow regime may be qualitatively different (Li and Zhang 2021). As Figs.1(a)-(c) show, when the ratio of the pore radius  $R$  to the thickness  $h_{bf}$  of the adsorbed layer potentially fully formed on the pore wall is over 100, the adsorbed layer effect is negligible and the flow can be wholly considered as macroscopic and continuum; when  $1 < R/h_{bf} < 100$ , the non-continuum adsorbed layer flow and the continuum liquid flow simultaneously occur, and the flow is thus essentially multiscale; when  $R/h_{bf} \leq 1$ , the continuum liquid vanishes and the flow is wholly non-continuum. The water flow in these three flow regimes should respectively be described by different flow equations.

## 3. Flow equations for different flow regimes

### 3.1 For the macroscopic continuum flow

As shown in Fig.1(a), when  $R/h_{bf} \geq 100$ , the flow in the whole pore is macroscopic and continuum, and by omitting the wall slippage the classical hydrodynamic theory gives the total mass flow rate through the pore as:

$$q_{m,conv} = -\frac{\pi\rho R^4}{4\eta} \frac{\partial p}{\partial x}, \text{ for } R/h_{bf} \geq 100 \quad (1)$$

where  $\rho$  and  $\eta$  are respectively the bulk density and bulk viscosity of the liquid,  $p$  is the pressure driving the liquid flow, and  $x$  is the coordinate in the axial direction.

### 3.2 For the multiscale flow

As Fig. 1(b) shows, when  $1 < R/h_{bf} < 100$ , the flow in the pore is essentially multiscale. Two models are required to respectively describe the molecular-scale non-continuum adsorbed layer flow and the intermediate continuum water flow. Classical multiscale approaches used molecular dynamics simulation to model the adsorbed layer flow and used the Newtonian fluid model to simulate the intermediate continuum liquid flow (Atkas and Aluru 2002; Yen *et al.* 2007). However, they can only simulate the multiscale flow in the small pore with a very small axial length normally no more than 100nm by using the advanced computer. Other multiscale approaches for solving the problem of the computational capacity may involve the use of the dissipative particle dynamics method (Kasiteropoulou *et al.* 2012, 2016, Perdikaris *et al.* 2016). Nevertheless, they are still required to use a huge number of particles for simulating the flow in a big area, and this should also cause the heavy computational burden. In recent years, Zhang (2020) used the non-continuum constitutive model to describe the adsorbed layer flow and used the Newtonian fluid model to describe the intermediate continuum liquid

flow. The advantage of his model is that it can simulate the realistic multiscale flow in the long pore with the axial length on the 0.1 $\mu\text{m}$  to 10mm scales just with the normal computational time and computer storage. Based on his model, by considering the liquid-pore wall interfacial slippage the total mass flow rate through the pore in Fig. 1(b) was derived by Zhang to be:

$$q_m = 2\pi R_{e,0} \bar{u} h_{bf} \rho_{bf,1}^{eff} + \pi \bar{u} (R - h_{bf})^2 \rho + 2\pi R_{e,0} \left[ \frac{F_1 h_{bf}^3}{12 \eta_{bf,1}^{eff}} \frac{\partial p}{\partial x} - \frac{h_{bf}^3}{2 \eta_{bf,1}^{eff}} \frac{\partial p}{\partial x} \left( 1 + \frac{1}{2 \lambda_{bf,0}} - \frac{q_0 - q_0^n}{q_0^{n-1} - q_0^n} \frac{\Delta_{n-2}}{h_{bf}} \frac{\varepsilon}{1 + \frac{\Delta x}{D}} \right) \rho_{bf,1}^{eff} + \left\{ \frac{F_2 \lambda_{bf,0}^2}{\eta_{bf,1}^{eff}} - \frac{\lambda_{bf,0}}{1 + \frac{\Delta x}{D}} \left( \frac{1}{2} + \lambda_{bf,0} - \frac{(q_0 - q_0^n) \Delta_{n-2}}{2(q_0^{n-1} - q_0^n)(R - h_{bf})} \right) \right\} \cdot \pi \rho (R - h_{bf})^4 \frac{\partial p}{\partial x} \right], \text{ for } 1 < R/h_{bf} < 100 \quad (2)$$

where  $\bar{u}$  is the interfacial slipping velocity on the adsorbed layer-pore wall interface,  $D$  is the diameter of the fluid molecule,  $R_{e,0} = R(1 - \lambda_x/2)$ ,  $\lambda_{bf,0} = \lambda_x/[2(1 - \lambda_x)]$ ,  $\lambda_x = h_{bf}/R$ ,  $\rho_{bf,1}^{eff}$  and  $\eta_{bf,1}^{eff}$  are respectively the average density and the effective viscosity of the adsorbed layer across the layer thickness,  $\eta_{bf,1}^{eff} = Dh_{bf}/[(n-1)(D + \Delta_x)(\Delta_l/\eta_{line,l})_{avr,n-1}]$ ,  $q_0 = \Delta_{j+1}/\Delta_j$  and  $q_0$  is constant,  $\Delta x$  is the separation between the neighboring liquid molecules in the flow direction in the adsorbed layer,  $\varepsilon = (2DI + II)/[h_{bf}(n-1)(\Delta_l/\eta_{line,l})_{avr,n-1}]$ ,  $F_1 = \eta_{bf}^{eff} (12D^2\psi + 6D\phi)/h_{bf}^3$ , and  $F_2 = 6\eta_{bf}^{eff} D(n-1)(\Delta_{l-1}/\eta_{line,l-1})_{avr,n-1}/h_{bf}^2$ ; Here,  $I = \sum_{i=1}^{n-1} i(\Delta_l/\eta_{line,l})_{avr,i}$ ,  $II = \sum_{i=0}^{n-2} [i(\Delta_l/\eta_{line,l})_{avr,i} + (i+1)(\Delta_l/\eta_{line,l})_{avr,i+1}] \Delta_i$ ,  $\psi = \sum_{i=1}^{n-1} i(\Delta_{l-1}/\eta_{line,l-1})_{avr,i}$ ,  $\phi = \sum_{i=0}^{n-2} [i(\Delta_{l-1}/\eta_{line,l-1})_{avr,i} + (i+1)(\Delta_{l-1}/\eta_{line,l-1})_{avr,i+1}] \Delta_i$ ,  $n$  is the equivalent number of the liquid molecules across the adsorbed layer thickness,  $\eta_{line,j-1}$  and  $\Delta_{j-1}$  are respectively the local viscosity and the separation between the  $j^{th}$  and  $(j-1)^{th}$  molecules across the adsorbed layer thickness, and  $j$  and  $(j-1)$  are respectively the order numbers of the molecules across the adsorbed layer thickness shown in Fig. 1(b).

For  $R/h_{bf} \geq 100$ , Eq. (2) is actually also valid. However, for this case the multiscale effect is weak so that the adsorbed layer effect is negligible, and Eq. (2) is reduced to the macroscopic continuum hydrodynamic flow equation.

According to the interfacial limiting shear strength model for the wall slippage (Zhang 2014), when the wall slippage occurs, the pressure drop on the axial length of the pore was derived by Zhang to be:

$$DP = \frac{l\tau_s}{R - h_{bf} + D(n-1)} \quad (3)$$

where  $\tau_s$  is the shear strength of the adsorbed layer-pore wall interface, and  $l$  is the axial length of the pore.

When the power loss on the whole pore for driving the flow is larger than the critical one, the wall slippage occurs. This critical power loss was derived by Zhang to be:

$$POW_{cr} = \frac{K_{cr} l (\tau_s h_{bf})^2}{\eta} \quad (4)$$

where

$$K_{cr} = \left[ \frac{1}{2\lambda_{bf,0} \left( 1 + \frac{D(n-1)}{R - h_{bf}} \right)} \right]^2 \left\{ 2\pi \frac{R_{e,0}}{R - h_{bf}} \left\{ \frac{4\varepsilon \lambda_{bf,0}^3}{C_{y,1} \left( 1 + \frac{\Delta x}{D} \right)} \left[ 1 + \frac{1}{2\lambda_{bf,0}} - \frac{\Delta_{n-2}(q_0 - q_0^n)}{h_{bf}(q_0^{n-1} - q_0^n)} \right] - \frac{2F_1 \lambda_{bf,0}^3}{3C_{y,1}} \right\} + \frac{\pi}{4} - \frac{4\pi}{C_{y,1}} \left[ \frac{F_2 \lambda_{bf,0}^2}{6} - \frac{\lambda_{bf,0}}{1 + \frac{\Delta x}{D}} \left[ \frac{1}{2} + \lambda_{bf,0} - \frac{\Delta_{n-2}(q_0 - q_0^n)}{2(R - h_{bf})(q_0^{n-1} - q_0^n)} \right] \right] \right\} \quad (5)$$

Here,  $C_{y,1} = \eta_{bf,1}^{eff}/\eta$ .

The power loss on the whole pore for driving the flow is equated as:  $POW = |DP q_v|$ , where  $q_v$  is the total volume flow rate through the pore and is related by the formula to the wall slipping velocity  $\bar{u}$ .

Based on the interfacial limiting shear strength model, the wall slipping velocity  $\bar{u}$  was derived by Zhang to be:

$$\bar{u} = \frac{DPOW[R - h_{bf} + D(n-1)]}{\pi \tau_s l [2R_{e,0} h_{bf} + (R - h_{bf})^2]} \quad (6)$$

where  $DPOW = POW - POW_{cr}$ . Eq. (6) shows that the wall slipping velocity  $\bar{u}$  is directly proportional to the value of  $DPOW$ . In molecular dynamics simulation, the slipping velocity  $\bar{u}$  on the wall of the carbon nanotube was directly calculated, and it is just the ensemble averaged velocity of the water molecule on the nanotube wall (Thomas *et al.* 2010).

As shown by Eq. (2), in the present multiscale model the wall slippage is incorporated by introducing the wall slipping velocity  $\bar{u}$ . Eq. (6) shows that the magnitude of the wall slippage i.e., the value of the wall slipping velocity  $\bar{u}$  is determined by the value of  $DPOW$ . In the present study,  $DPOW$  is widely varied to give different magnitudes of the wall slippage.

When the wall slippage occurs, the total volume flow rate through the pore was calculated by Zhang to be:

$$q_v = \frac{C_1 POW}{\tau_s}, \text{ for } POW > POW_{cr} \quad (7)$$

where

$$C_1 = \frac{h_{bf}}{l} \left[ 1 + \frac{1}{2\lambda_{bf,0}} - \frac{1 + \frac{\Delta_{n-2}(q_0 - q_0^n)}{D(q_0^{n-1} - q_0^n)}}{2\lambda_{bf,0} \frac{R - h_{bf}}{D}} \right] \quad (8)$$

By ignoring the adsorbed layer, the classical macroscopic continuum hydrodynamic flow theory gives the total volume flow rate through the pore as:

$$q_{v,conv} = \frac{R^2}{2} \sqrt{\frac{\pi POW}{\eta l}} \quad (9)$$

For the hydrophobic pore wall, owing to the weak liquid-pore wall interaction, the solidification of the adsorbed layer is weak and the average density of the adsorbed layer is nearly equal to the bulk density of the liquid. Thus, the ratio of the total mass flow rate through the pore of the multiscale flow to that calculated from the classical hydrodynamic flow theory is:

$$r_m = \frac{q_v}{q_{v,conv}} \quad (10)$$

### 3.3 For the non-continuum nanoscale flow

For  $R/h_{bf} \leq 1$ , the continuum liquid vanishes in the pore and the flow in the pore is wholly non-continuum as Fig. 1(c) shows. For this case, the total mass flow rate through the pore is (Zhang 2017):

$$q_m = \pi \rho_{bf,2}^{eff} u_s R^2 + \frac{\pi \rho_{bf,2}^{eff} S R^4}{4 \eta_{bf,2}^{eff}} \frac{\partial p}{\partial x} \quad (11)$$

where  $u_s$  is the slipping velocity on the pore wall,  $\rho_{bf,2}^{eff}$  and  $\eta_{bf,2}^{eff}$  are respectively the average density and the effective viscosity of the non-continuum film in the whole pore, and  $S$  is the parameter accounting for the non-continuum effect of the film.

Eq. (11) takes into account the variations of both the local density and the local viscosity across the radius of the nanopore as MDS revealed. It also incorporates the non-continuum effect due to the discontinuity and inhomogeneity across the nanopore radius by using the parameter  $S$  ( $-1 < S < 0$ ) (Zhang 2013a, b, 2015a, 2016a). The present non-continuum flow model well matches the MDS results (Jiang and Zhang 2022, Zhang 2015a, b, 2016a, b, c, 2018, 2019).

According to the interfacial limiting shear strength model for the wall slippage, when the wall slippage occurs, the pressure drop on the axial length of the pore is:

$$DP = \frac{\tau_s l}{\theta_\tau R} \quad (12)$$

where  $\theta_\tau$  is the correction factor for the shear stress on the pore wall owing to the non-continuum effect of the film.

The critical power loss on the whole pore for initiating the wall slippage is:

$$POW_{cr} = -\left(\frac{\tau_s}{\theta_\tau}\right)^2 \frac{\pi S R^2 l}{4 \eta_{bf,2}^{eff}} \quad (13)$$

The ratio of the total mass flow rate through the pore to that calculated from the classical hydrodynamic flow theory is:

$$r_m = \frac{4 C_{q,2} \theta_\tau^2 \eta (DPOW)}{\pi R^2 \tau_s^2 l} - \frac{C_{q,2} S}{C_{y,2}} \quad (14)$$

where  $C_{y,2} = \eta_{bf,2}^{eff} / \eta$ ,  $C_{q,2} = \rho_{bf,2}^{eff} / \rho$  and  $DPOW = POW - POW_{cr}$ .

## 4. Calculation

The calculation was made for the water flow in the carbon micro/nano tubes for widely varying values of  $R$  covering the multiscale flow and the non-continuum

nanoscale flow. There is a quite weak interaction between the water and the carbon wall. The carbon nanotube is highly hydrophobic showing the very low friction behavior to the water flow. The input parameter values were chosen as follows:

$$D=0.28\text{nm}, \eta = 0.001\text{Pa} \cdot \text{s}, \tau_s = 0.02\text{kPa}, \Delta x/D = \Delta_{n-2}/D = 0.15, n = 3, q_0 = 1.01, l = 1000\text{nm}$$

It was taken that  $\eta_{line,i}/\eta_{line,i+1} = q_0^{0.2}$ . The value of  $h_{bf}$  was calculated to be 0.924nm.

The parameter  $C_{y,1}$  is expressed as (Zhang 2004):

$$C_{y,1}(H_{bf}) = 0.9507 + \frac{0.0492}{H_{bf}} + \frac{1.6447E-4}{H_{bf}^2} \quad (15)$$

where  $H_{bf} = h_{bf}/h_{cr}$ , and  $h_{cr}$  is the critical thickness for characterizing the influence of the adsorbed layer thickness on the effective viscosity of the adsorbed layer; here,  $h_{cr} = 1.4\text{nm}$ .

The parameter  $C_{y,2}$  is expressed as (Zhang 2004):

$$C_{y,2}(\bar{R}) = 0.9507 + \frac{0.0492}{\bar{R}} + \frac{1.6447E-4}{\bar{R}^2}, \quad (16)$$

for  $0.1 < \bar{R} < 1.0$

where  $\bar{R} = R/R_{cr}$ , and  $R_{cr}$  is the critical radius for characterizing the influence of the pore radius on the effective viscosity and average density of the non-continuum film in the whole pore (Meyer *et al.* 1998). For  $R = R_{cr}$ ,  $C_{y,2} = 1$ , and the effective viscosity of the water film in the pore is equal to the water bulk viscosity. Here,  $R_{cr} = 2h_{cr} = 2.8\text{nm}$ .

The other parameters are formulated as (Zhang 2004):

$$C_{q,2}(\bar{R}) = 1.116 - 0.328\bar{R} + 0.253\bar{R}^2 - 0.041\bar{R}^3, \quad (17)$$

for  $0.1 < \bar{R} < 1.0$

$$S(\bar{R}) = [-0.1 - 0.892(\bar{R} - 0.1)^{-0.084}]^{-1}, \quad (18)$$

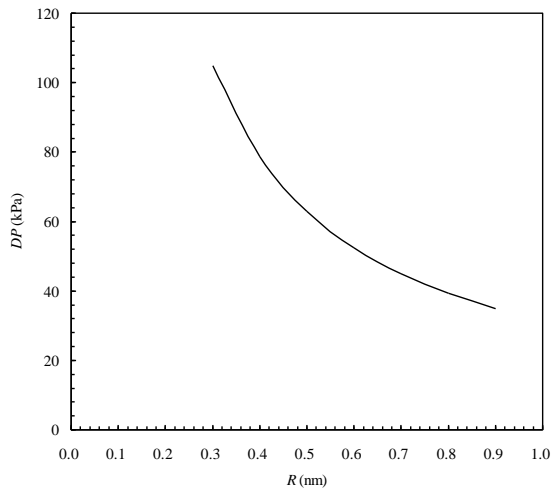
for  $0.1 < \bar{R} < 1.0$

For  $R = R_{cr}$ ,  $C_{q,2} = 1$  and  $S = -1$ . For this case, the average density of the water film in the pore is equal to the water bulk density, and the non-continuum effect on the Poiseuille flow of water vanishes and Eq. (11) becomes conventional if  $u_s = 0$  (for the non-continuum effect,  $-1 < S < 0$ ).

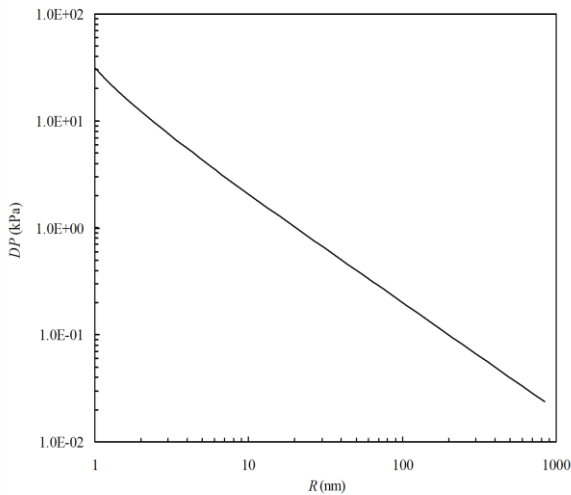
## 5. Results

Figs. 2(a) and (b) show the values of the pressure drop  $DP$  on the micro/nano tubes with the axial length  $l = 1000\text{nm}$  for widely varying pore radius when the wall slippage occurs and the flow in the pore is respectively non-continuum nanoscale and multiscale. For the continuity of  $DP$ , it was taken that  $\theta_\tau = 0.636$ . For the wall slippage occurrence, the value of  $DP$  is significantly increased with the reduction of  $R$ .

Figs. 3(a)-(c) show the critical power losses ( $POW_{cr}$ ) on the micro/nano tubes with the axial length  $l = 1000\text{nm}$  for initiating the wall slippage for different pore radii ( $R$ ) when the flow in the pore is respectively non-continuum



(a)

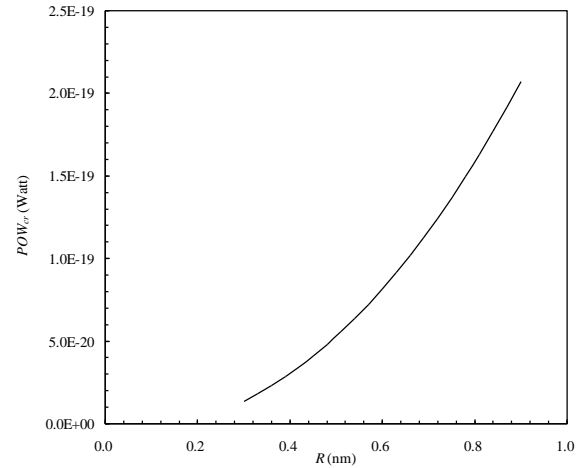


(b)

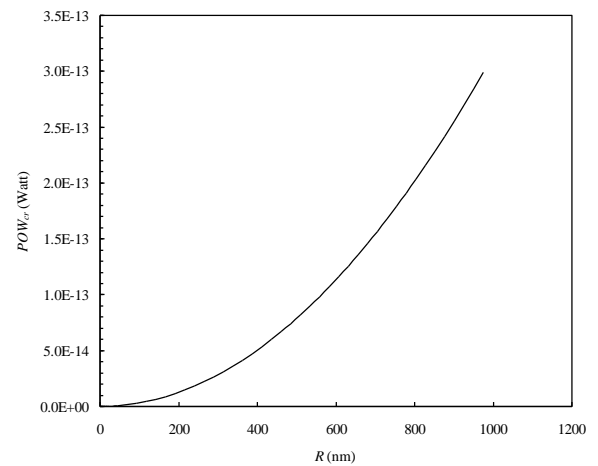
Fig. 2 Pressure drops on the micro/nano tubes with the axial length  $l = 1000\text{nm}$  for widely varying pore radius when the wall slippage occurs. (a) In the non-continuum nanoscale flow; (b) In the multiscale flow.

nanoscale and multiscale. The value of  $POW_{cr}$  is rapidly reduced with the reduction of  $R$ ; for  $R \leq 0.9\text{nm}$ , the value of  $POW_{cr}$  is no more than  $2.0\text{E-}19\text{Watt}$ . These mean that in the carbon nanotube with the diameter no more than  $1.8\text{nm}$  the wall slippage very easily occurs just with a very tiny power driving the water flow. This well correlates with the experimental observations of the water flow through the carbon nanotube with the diameter below  $2\text{nm}$  by Holt *et al.* (2006) and Qin *et al.* (2011) which were attributed to the great wall slippage. Majumder *et al.* (2005) also noticed the significant wall slippage for the water flow through the carbon nanotube with the diameter below  $7\text{nm}$ .

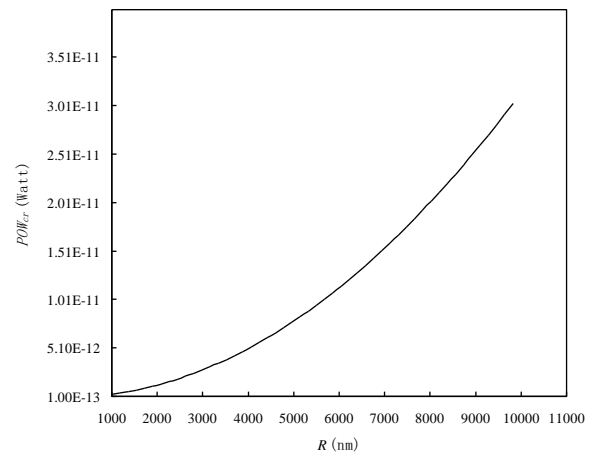
Figs. 4(a)-(c) show the calculated values of the ratio  $r_m$  of the mass flow rate through the pore in the condition of the wall slippage or no wall slippage to that calculated from the classical macroscopic flow theory. For no wall slippage ( $DPOW = 0$ ), the water flow rate through the pore in the multiscale flow regime (for  $R \geq 1\text{nm}$ ) can be calculated



(a)



(b)



(c)

Fig. 3 Critical power loss on the micro/nano tubes with the axial length  $l = 1000\text{nm}$  for initiating the wall slippage, as function of the pore radius  $R$ . (a) In the non-continuum nanoscale flow; (b), (c) In the multiscale flow

from the classical macroscopic hydrodynamic flow theory since  $r_m$  is very close to unity; however in the non-continuum nanoscale flow regime, the water flow rate through the pore is considerably smaller than the classical

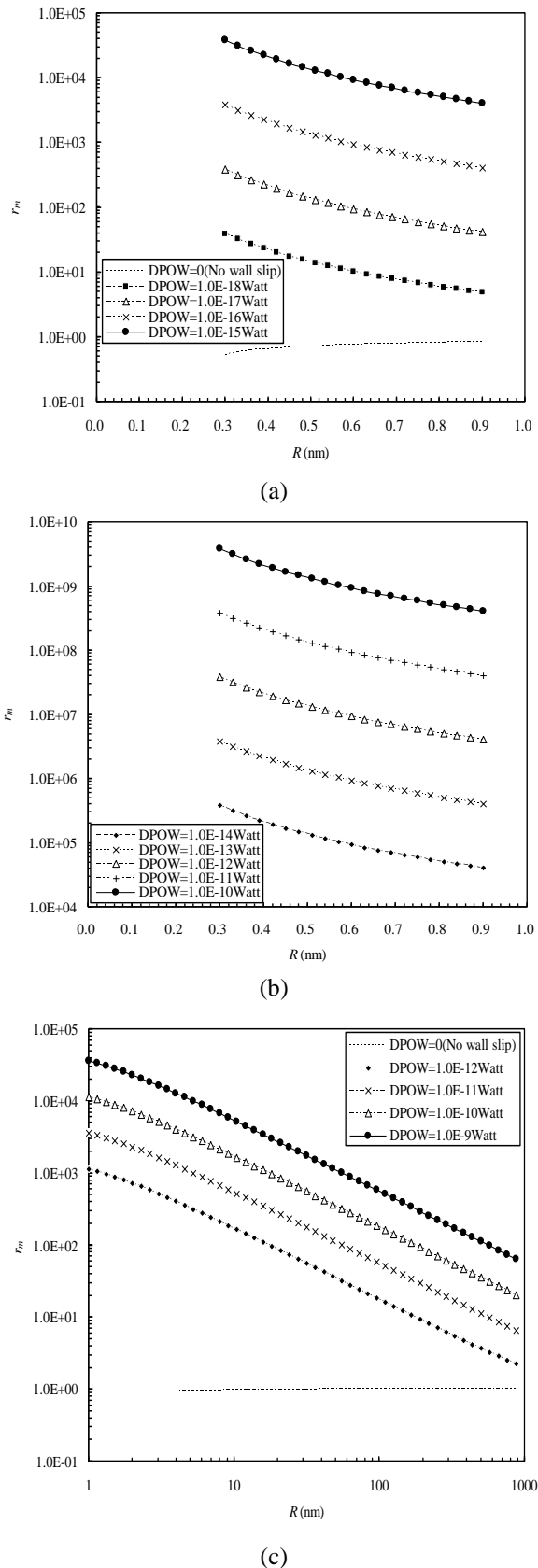


Fig. 4 Ratio of the mass flow rate through the pore in the condition of the wall slippage or no wall slippage to that calculated from the classical macroscopic flow theory. (a), (b) In the non-continuum nanoscale flow; (c) In the multiscale flow

macroscopic hydrodynamic flow theory calculation when  $R < 0.5\text{nm}$ , this is due to the pronounced non-continuum effect of the water film, which significantly impedes the Poiseuille flow (Zhang 2017). When the wall slippage occurs (i.e.,  $DPOW > 0$ ), for the pore diameter below  $1.8\text{nm}$  i.e. the non-continuum nanoscale flow, the values of  $r_m$  cover the range from  $10^1$  to  $10^{10}$  when  $DPOW$  is increased from  $1.0\text{E-}18\text{Watt}$  to  $1.0\text{E-}10\text{Watt}$ . These water flow enhancements cover the water flow enhancement ranges found in the experiments by Holt *et al.* (2006) and Qin *et al.* (2011) for the carbon nanotubes with the diameters below  $2.0\text{nm}$ . There are the discrepancies between the experimental results of the water flow enhancements respectively obtained by Holt *et al.* (2006) and Qin *et al.* (2011). Consequently, there have been the disputes about these discrepancies, some of which ascribed to the entry and exit pressure losses (Walther *et al.* 2013) while others ascribed to different slip lengths (Kannam *et al.* 2013). However, even for the long carbon nanotubes, where the influence of the entry and exit pressure losses should be negligible, there are still the discrepancies between the experimental results of Holt *et al.* (2006) and Qin *et al.* (2011). The present calculation results apparently indicate that the water flow enhancement in the carbon nanotube is severely dependent on the power loss on the whole nanotube which drives the water flow. A different power loss gives quite a different water flow enhancement factor. This finding was omitted by all the previous researches (Holt *et al.* 2006, Kannam *et al.* 2013, Qin *et al.* 2011, Walther *et al.* 2013). The present results also strongly indicate that smaller the nanopore diameter, easier the wall slippage, and greater the water flow enhancement. These results agree with the experiments (Holt *et al.* 2006, Qin *et al.* 2011, Secchi *et al.* 2016). It is shown that even a very tiny power loss ( $1.0\text{E-}14\text{Watt}$ ~ $1.0\text{E-}10\text{Watt}$ ) on the whole carbon nanotube with the diameter below  $1.8\text{nm}$  generates the wall slippage which results in the huge water flow enhancement (with the orders 5 to 9).

Fig. 4 (c) shows that for a given  $DPOW$ , when the pore radius is increased from  $1\text{nm}$  to  $1000\text{nm}$ , the value of  $r_m$  (i.e. the water flow enhancement factor) is reduced by two orders. This shows the great influence of the pore diameter on the water flow enhancement in carbon nanotubes, fairly agreeing with the experiments (Holt *et al.* 2006, Qin *et al.* 2011, Secchi *et al.* 2016). Even for  $R = 1000\text{nm}$ , the water flow enhancement is by two orders for  $DPOW = 1.0\text{E-}9\text{Watt}$ . These show the fact of the very easy occurrence of the water film slippage in carbon micro/nanotubes which largely contributes to the water flow enhancement.

Table 1 shows the values of the water flow enhancement factors in carbon nanopores with different diameters experimentally or analytically obtained by different research groups. The experimental results from different researchers are quite divergent even for the same diameter ranges. The recognition of such a divergence is still not reconciled with a lot of explanations. The present calculation results cover all the experimental results, strongly indicating the heavy dependence of the flow enhancement factor on the power loss on the whole nanopore for driving the water flow.

Table 1 Water flow enhancement factors in carbon nanopores obtained by experiments or calculations

Nanopore diameter (nm)	Flow enhancement factor
300-500	$\approx 1$ (Exp. by Ray <i>et al.</i> (2009))
44	22 (Exp. by Whitby <i>et al.</i> (2008))
7	44000-77000 (Exp. by Majumder <i>et al.</i> (2005))
	$\sim 500$
1.6-5	$\sim 100$
5-10	1-10
>10	(MDS by Thomas <i>et al.</i> (2010))
1.66-4.99	50-430 (Exp. by Thomas and McGaughey (2009))
1.3-2.0	560-8400 (Exp. by Holt <i>et al.</i> (2006))
0.81-1.66	430-6500 (Exp. by Thomas and McGaughey (2009))
0.81-1.59	51-882 (Exp. by Qin <i>et al.</i> (2011))
0.6-1.8	$10-10^9$ (dependent on the value of <i>DPOW</i> )
2.0-2000	$1-10^4$ (dependent on the value of <i>DPOW</i> ) (Present calculation)

## 6. Conclusions

The ratio of the mass flow rate through the micro/nano cylindrical pores with different radii to that calculated from the classical macroscopic hydrodynamic flow theory is calculated when the wall slippage occurs or not. The non-continuum nanoscale flow equation or the multiscale flow equation were used when the pore diameter was varied so that the flow regime in the pore was changed. The calculation was made specifically for the water flow in the carbon micro/nano tubes with widely varying inner diameters. The obtained water flow enhancement factors in the carbon nanotubes cover the range of the experimental measurements and strongly indicate the contribution of the wall slippage to the ultra fast water flow in carbon nanotubes. The results are of significant interest to the water filtration by using micro/nano porous membranes. The important conclusions are drawn as follows:

- For no wall slippage, the water mass flow rate through the carbon micro/nano tubes with the diameters over 1.0nm can be calculated from the classical macroscopic hydrodynamic flow theory; For the pore diameter below 1.0nm, the water mass flow rate through the pore is considerably smaller than the classical macroscopic hydrodynamic flow theory calculation owing to the non-continuum effect of the water film.

- The wall slippage easily occurs when water flows through the carbon micro/nano tubes even with the diameter on the scales of 1 “ $\mu\text{m}$ ” or 10 “ $\mu\text{m}$ ”. Smaller the pore diameter, lower the critical power loss on the whole pore for initiating the wall slippage, and easier the wall slippage. For the pore diameter on the 1nm scale, even a very tiny power loss on the whole pore such as on the scale of 1.0E-18Watt can generate the significant wall slippage, which results in the water flow enhancement by 1~2 orders.

- The water flow enhancement in carbon micro/nano tubes due to the wall slippage not only strongly depends on the pore diameter but also severely depends on the power loss on the whole pore for driving the flow.

## Acknowledgments

Dr. Wang would like to express thanks to the support from the Natural Science Project of Changzhou College of Information Technology with the project number CXZK202104Y.

## References

- Atkas, O. and Aluru, N.R. (2002), “A combined continuum/DSMC technique for multiscale analysis of microfluidic filters”, *J. Comput. Phys.*, **178**, 342-372.  
<https://doi.org/10.1006/jcph.2002.7030>
- Azamat, J. (2021), “Application of graphene, graphene oxide, and boron nitride nanosheets in the water treatment”, *Membr. Water Treat.*, **12**, 227-243.  
<https://doi.org/10.12989/mwt.2021.12.5.227>
- Borg, M.K. and Reese, J.M. (2017), “Multiscale simulation of enhanced water flow in nanotubes”, *MRS Bulletin*, **42**, 294-299.  
<https://doi.org/10.1557/mrs.2017.59>
- Calabrò, F., Lee, K.P. and Mattia, D. (2013), “Modelling flow enhancement in nanochannels: Viscosity and slippage”, *Appl. Math. Lett.*, **26**, 991-994.  
<https://doi.org/10.1016/j.aml.2013.05.004>
- Das, D., Kayal, N., and Innocentini, M.D.M. (2021), “Effect of processing parameters on mullite bonded SiC membrane for turbid water filtration”, *Membr. Water Treat.*, **12**(3), 133-138.  
<https://doi.org/10.12989/mwt.2021.12.3.133>
- Dai, H., Xu, Z., and Yang, X. (2016), “Water permeation and ion rejection in layer-by-layer stacked graphene oxide nanochannels: A molecular dynamics simulation”, *J. Phys. Chem.*, **120**, 22585-22596. <https://doi.org/10.1021/acs.jpcc.6b05337>
- Gruener, S., Wallacher, D., Greulich, S., Busch, M. and Huber, P. (2016), “Hydraulic transport across hydrophilic and hydrophobic nanopores: Flow experiments with water and n-hexane”, *Phys. Rev.*, **93**, 013h102.  
<https://doi.org/10.1103/PhysRevE.93.013102>
- Holt, J.K., Park, H.G., Wang, Y., Stadermann, M., Artyukhin, A. B., Grigoropoulos, C.P., Noy, A. and Bakajin, O. (2006), “Fast mass transport through sub-2-nanometer carbon nanotubes”, *Science*, **312**, 1034-1037.  
<https://doi.org/10.1126/science.1126298>
- Itoh, Y., Chen, S., Hirahara, R., Konda, T., Aoki, T., Ueda, T., Shimada, I., Cannon, J.J., Shao, C., Shiomi, J., Tabata, K.V., Noji, H., Sato, K., and Aida, T. (2022), “Ultrafast water permeation through nanochannels with a densely fluorinated interior surface”, *Science*, **376**, 738-743.  
<https://doi.org/10.1126/science.abd0966>
- Jiang, C.T. and Zhang, Y.B. (2022), “Direct matching between the flow factor approach model and molecular dynamics simulation for nanochannel flows”, *Sci. Rep.*, **12**, 396.  
<https://doi.org/10.1038/s41598-021-04391-5>
- Kannam, S.K., Todd, B.D., Hansen, J.S. and Daivis, P.J. (2013), “How fast does water flow in carbon nanotubes?”, *J. Chem. Phys.*, **138**, 094701. <http://doi.org/10.1063/1.4793396>
- Kasiteropoulou, D., Karakasidis, T.E. and Liakopoulos, A. (2012), “A dissipative particle dynamics study of flow in periodically grooved nanochannels”, *Int. J. Num. Meth. Fluids*, **68**, 1156-1172. <https://doi.org/10.1002/fld.2599>
- Kasiteropoulou, D., Karakasidis, T.E. and Liakopoulos, A. (2016), “Study of fluid flow in grooved micro and nano-channels via dissipative particle dynamic: a tool for desalination membrane design”, *Desal. Water Treat.*, **57**, 11675-11684.  
<https://doi.org/10.1080/19443994.2016.1141118>
- Li, J. and Zhang, Y.B. (2021), “Flow equations and their borderlines for different regimes of mass transfer”, *Front. Heat*

- Mass Transf.*, **16**, 21. <http://doi.org/10.5098/hmt.16.21>
- Majumder, M., Chopra, N., Andrews, R. and Hinds, B.J. (2005), "Enhanced flow in carbon nanotubes", *Nature*, **438**, 44. <https://doi.org/10.1038/438044a>
- Mattia, D. and Calabro, F. (2012), "Explaining high flow rate of water in carbon nanotubes via solid-liquid molecular interactions", *Microfluid. Nanofluid.*, **13**, 125-130. <https://doi.org/10.1007/s10404-012-0949-z>
- Meyer, E., Overney, R.M., Dransfeld, K., Gyalog, T. (1998), *Friction and Rheology on the Nanometer Scale*. World Scientific Press, New Jersey, U.S.A.
- Myers, T.G. (2011), "Why are slip lengths so large in carbon nanotubes?" *Microfluid. Nanofluid.*, **10**, 1141-1145. <https://doi.org/10.1007/s10404-010-0752-7>
- Perdikaris, P., Grinberg, L. and Karniadakis, G.E. (2016), "Multiscale modeling and simulation of brain blood flow", *Phys. Fluids*, **28**, 021304. <https://doi.org/10.1063/1.4941315>
- Qin, X.C., Yuan, Q., Zhao, Y., Xie, S. and Liu, Z. (2011), "Measurement of the rate of water translocation through carbon nanotubes", *Nano Lett.*, **11**, 2173-2177. <https://doi.org/10.1021/nl200843g>
- Radhal, A. Esfandiari, F., Wang, A.P., Rooney, K., Gopinadhan, A., Keerthi, A., Mishchenko, A., Janardanan, P., Fumagalli, M., Lozada-Hidalgo, S., Garaj, S.J., Haigh, I.V., Grigorieva, H.A., and Wu, A.K. (2016), "Molecular transport through capillaries made with atomic-scale precision", *Nature*, **538**, 222-225. <https://doi.org/10.1038/nature19363>
- Ray, S.S., Chando, P. and Yarin, A.L. (2009), "Enhanced release of liquid from carbon nanotubes due to entrainment by an air layer", *Nanotechnology*, **20**, 095711. <https://doi.org/10.1088/0957-4484/20/9/095711>
- Ritos, K., Mattia, D., Calabro, F. and Reese, J. M. (2014), "Flow enhancement in nanotubes of different materials and lengths", *J. Chem. Phys.*, **140**, 014702. <https://doi.org/10.1063/1.4846300>
- Secchi, E., Marbach, S., Niguès, A., Stein, D., Siria, A. and Bocquet, L. (2016), "Massive radius-dependent flow slippage in carbon nanotubes", *Nature*, **537**, 210-213. <https://doi.org/10.1038/nature19315>
- Thomas, J.A. and McGaughey, A.J.H. (2008), "Density, distribution, and orientation of water molecules inside and outside carbon nanotubes", *J. Chem. Phys.*, **128**, 084715. <https://doi.org/10.1063/1.2837297>
- Thomas, J.A. and McGaughey, A.J.H. (2009), "Water flow in carbon nanotubes: Transition to subcontinuum transport", *Phys. Rev. Lett.*, **102**, 184502. <https://doi.org/10.1103/PhysRevLett.102.184502>
- Thomas, J.A., McGaughey, A.J.H. and Kuter-Arnebeck, O. (2010), "Pressure-driven water flow through carbon nanotubes: Insights from molecular dynamics simulation", *Int. J. Therm. Sci.*, **49**, 281-289. <https://doi.org/10.1016/j.ijthermalsci.2009.07.008>
- Walther, J.H., Ritos, K., Cruz-Chu, E.R., Megaridis, C.M. and Koumoutsakos, P. (2013), "Barriers to superfast water transport in carbon nanotube membranes", *Nano Lett.*, **13**, 1910-1914. <https://doi.org/10.1021/nl304000k>
- Whitby, M. and Quirke, N. (2007), "Fluid flow in carbon nanotubes and nanopipes", *Nature Nanotechnology*, **2**, 87-94. <https://doi.org/10.1038/nnano.2006.175>
- Whitby, M.C., Cagno, L., Thanou, M. and Quirke, N. (2008), "Enhanced fluid flow through nanoscale carbon pipes", *Nano Lett.*, **8**, 2632-2637. <https://doi.org/10.1021/nl080705f>
- Yen, T.H., Soong, C.Y. and Tzeng, P.Y. (2007), "Hybrid molecular dynamics-continuum simulation for nano/mesoscale channel flows", *Microfluid. Nanofluid.*, **3**, 665-675. <https://doi.org/10.1007/s10404-007-0154-7>
- Zhang, Y.B. (2004), "Modeling of molecularly thin film elastohydrodynamic lubrication", *J. Balkan Trib. Assoc.*, **10**, 394-421.
- Zhang, Y.B. (2013a), "The Reynolds equation for boundary film considering the non-continuum effect and its application to the one-dimensional micro step bearing: Part I-Calculation for no boundary slippage", *J. Comput. Theor. Nanosci.*, **10**, 603-608. <https://doi.org/10.1166/jctn.2013.2742>
- Zhang, Y.B. (2013b), "The Reynolds equation for boundary film considering the non-continuum effect and its application to the one-dimensional micro step bearing: Part II-Calculation for boundary slippage", *J. Comput. Theor. Nanosci.*, **10**, 609-615. <https://doi.org/10.1166/jctn.2013.2742>
- Zhang, Y.B. (2014), "Review of hydrodynamic lubrication with interfacial slippage", *J. Balkan Trib. Assoc.*, **20**, 522-538.
- Zhang, Y.B. (2015a), "The flow factor approach model for the fluid flow in a nano channel", *Int. J. Heat Mass Transf.*, **89**, 733-742. <https://doi.org/10.1016/j.ijheatmasstransfer.2015.05.092>
- Zhang, Y.B. (2015b), "A quantitative comparison between the flow factor approach model and the molecular dynamics simulation results for the flow of a confined molecularly thin fluid film", *Theor. Comput. Fluid Dyn.*, **29**, 193-204. <https://doi.org/10.1007/s00162-015-0348-7>
- Zhang, Y.B. (2016a), "The flow equation for a nanoscale fluid flow", *Int. J. Heat Mass Transf.*, **92**, 1004-1008. <https://doi.org/10.1016/j.ijheatmasstransfer.2015.09.008>
- Zhang, Y. B. (2016b), "Calculating the maximum flowing velocity of the Poiseuille flow in a nano channel by the flow factor approach model", *Int. Commun. Heat Mass Transf.*, **73**, 111-113. <https://doi.org/10.1016/j.icheatmasstransfer.2016.02.014>
- Zhang, Y.B. (2016c), "An additional validation of the flow factor approach model", *Int. J. Heat Mass Transf.*, **95**, 953-955. <https://doi.org/10.1016/j.ijheatmasstransfer.2016.01.016>
- Zhang, Y.B. (2017), "Transport in nanotube tree", *Int. J. Heat Mass Transf.*, **114**, 536-540. <https://doi.org/10.1016/j.ijheatmasstransfer.2017.06.105>
- Zhang, Y.B. (2018), "Size effect on nanochannel flow explored by the flow factor approach model", *Int. J. Heat Mass Transf.*, **125**, 681-685. <https://doi.org/10.1016/j.ijheatmasstransfer.2018.04.064>
- Zhang, Y.B. (2019), "Density and viscosity profiles governing nanochannel flow", *Phys. A: Stat. Mech. Its Appl.*, **521**, 1-8. <https://doi.org/10.1016/j.physa.2019.01.079>
- Zhang, Y.B. (2020), "Modeling of flow in a very small surface separation", *Appl. Math. Mod.*, **82**, 573-586. <https://doi.org/10.1016/j.apm.2020.01.069>

CC